Old Dominion University
ODU Digital Commons

Mathematics & Statistics Faculty Publications

Mathematics & Statistics

3-2004

Astronaut EVA Exposure Estimates from CAD Model Spacesuit Geometry

Giovanni De Angelis
Old Dominion University

Brooke M. Anderson

William Atwell

John E. Nealy
Old Dominion University

Gary D. Qualls

See next page for additional authors

Original Publication Citation

De Angelis, G., Anderson, B. M., Atwell, W., Nealy, J. E., Qualls, G. D., & Wilson, J. W. (2004). Astronaut EVA exposure estimates from CAD model spacesuit geometry. *Journal of Radiation Research, 45*(1), 1-9. doi:10.1269/jrr.45.1

Authors
Giovanni De Angelis, Brooke M. Anderson, William Atwell, John E. Nealy, Gary D. Qualls, and John W. Wilson

J. Radiat. Res., 45, 1–9 (2004) *Regular Paper*

Astronaut EVA Exposure Estimates from CAD Model Spacesuit Geometry

Giovanni DE ANGELIS[1,2,3]*, Brooke M. ANDERSON[4], William ATWELL[5], John E. NEALY[1], Garry D. QUALLS[2] and John W. WILSON[2]

Space Radiation/EVA/LEO/ISS/Radiation Safety/Modeling.

Ongoing assembly and maintenance activities at the International Space Station (ISS) require much more extravehicular activity (EVA) than did the earlier U.S. Space Shuttle missions. It is thus desirable to determine and analyze, and possibly foresee, as accurately as possible what radiation exposures crew members involved in EVAs will experience in order to minimize risks and to establish exposure limits that must not to be exceeded. A detailed CAD model of the U.S. Space Shuttle EVA Spacesuit, developed at NASA Langley Research Center (LaRC), is used to represent the directional shielding of an astronaut; it has detailed helmet and backpack structures, hard upper torso, and multilayer space suit fabric material. The NASA Computerized Anatomical Male and Female (CAM and CAF) models are used in conjunction with the space suit CAD model for dose evaluation within the human body. The particle environments are taken from the orbit-averaged NASA AP8 and AE8 models at solar cycle maxima and minima. The transport of energetic particles through space suit materials and body tissue is calculated by using the NASA LaRC HZETRN code for hadrons and a recently developed deterministic transport code, ELTRN, for electrons. The doses within the CAM and CAF models are determined from energy deposition at given target points along 968 directional rays convergent on the points and are evaluated for several points on the skin and within the body. Dosimetric quantities include contributions from primary protons, light ions, and electrons, as well as from secondary brehmsstrahlung and target fragments. Directional dose patterns are displayed as rays and on spherical surfaces by the use of a color relative intensity representation.

INTRODUCTION

The radiation environment to which an astronaut is exposed during an EVA may contribute significantly to the cumulative exposure that may be experienced during extended missions.[1)] Mission scenarios to be considered include low earth orbit (LEO) and deep space. In LEO the main concern is trapped protons and electrons, and in deep space the particle fluxes because of Solar Particle Events (SPE) need to be evaluated. Although galactic cosmic rays (GCR) are important to be considered in long-term exposures, their intensity in a short time frame such as an EVA results only in a low-level background and is much less than that of a solar flare[2,3)]; therefore they will not be discussed further in this paper. It is important to study the dose gradients about the body during an EVA to help determine the radiation risk associated with the different environments.[2-6)] If the dose at a given target point is to be analytically determined, several items must be modeled. The first is the external environment that includes the radiation fields; the models used for this analysis will be discussed later. The second is the type of shielding material that will be provided. For this discussion, the materials will be the EVA space suit and the human tissue surrounding a given target point within the body. For the modeling of the human body, the Computerized Anatomical Male and Female (CAM and CAF) data sets[7,8)] will be used in environmental assessments and in health-based procedures for an evaluation of the radiation health-related quantities.[9,10)] How the suit material is modeled is described in a following section.

SPACE SUIT CAD MODEL

To be suitable for radiation-related analyses, a model should provide a description of masses, thickness, volumes, and materials and their elemental composition. The brief description here is taken largely from Refs. 1 and 11, and the major space suit components are shown in Fig. 1. For the Shuttle EVA space suit, the main components are the Hard Upper Torso (HUT), the arm assembly, the Lower Torso Assembly (LTA), extravehicular gloves, the helmet, the Primary Life Support System (PLSS) attached to the back of the suit, the Liquid Cooling and Ventila-

*Corresponding author: Phone: +1-757-864-1423,
Fax: 1-757-864-8094,
E-mail: g.deangelis@larc.nasa.gov
[1]Old Dominion University, Norfolk VA, 23508-0369, USA; [2]NASA Langley Research Center, Hampton VA, 23681-2199, USA; [3]Istituto Superiore di Sanita', Rome, I-00161, Italy; [4]Swales Aerospace Corporation, Hampton VA, 23681, USA; and [5]The Boeing Company, Houston TX, 77058, USA.

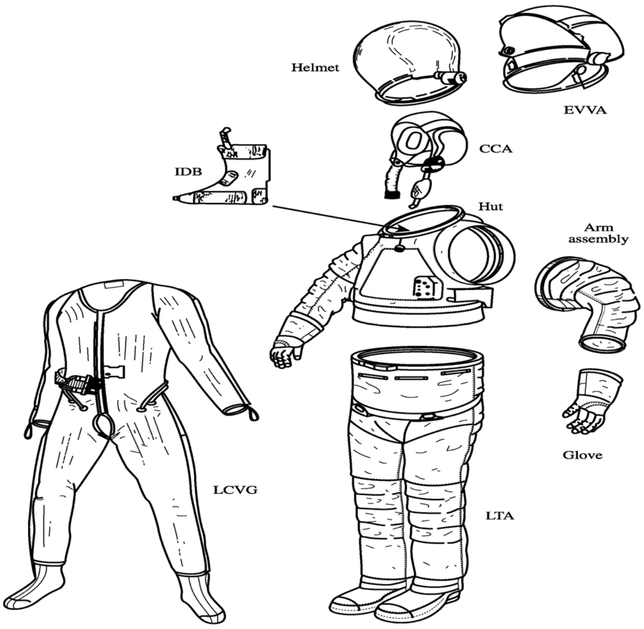

Fig. 1. Basic components of the U.S. Space Shuttle EVA spacesuit.[1]

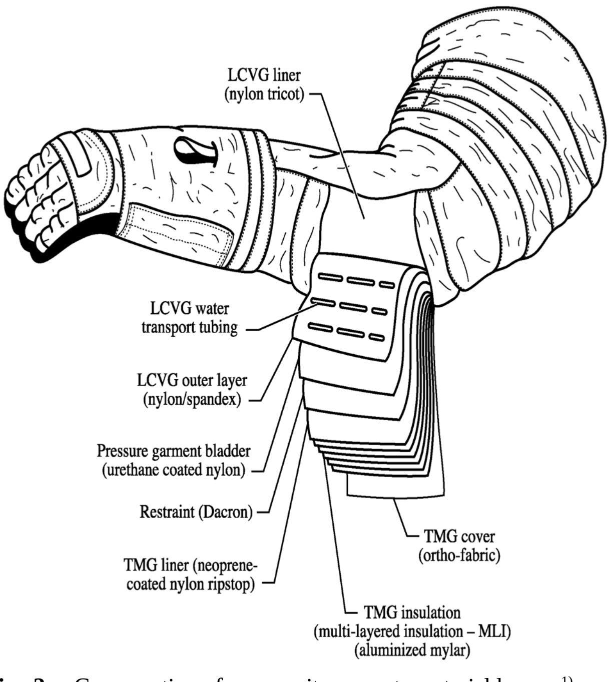

Fig. 2. Cross section of space suit garments material lay-up.[1]

tion Garment (LCVG) under the pressure suit and directly against the astronaut's body, and the Extra-Vehicular Visor Assembly (EVVA) over the helmet. The HUT is constructed of fiberglass and covered outside with orthofabric, aluminized Mylar, and neoprene-coated nylon ripstop. The LTA and arm assembly, including the LCVG, consists of orthofabric, aluminized Mylar, neoprene-coated ripstop, polyester, urethane-coated nylon, and water-filled cooling tubes, as shown in Fig. 2.

Table 1. Major material constituents and approximate masses of PLSS.

Subsystem	Material constituents	Mass (kg)
O_2 ventilating circuit		
Regulators, vessels, fans	Fe, Cr, Ni, Cu, etc.	6.5
LiOH assembly	LiOH, Fe	2.9
H_2O transport		
Pump, valves, sensors	Fe, Cu	2.9
Liquid	H_2O	2.0
Electrical system		
Electronics	Si, O, Cu, etc.	6.8
Battery	ZnAgO	4.5
O_2 purge system		
Bottles	Fe, O_2	3.9
Regulator	Fe	1.9

Table 2. Shuttle space suit helmet and EVVA constituents.

Component	Materials	Areal density (g/cm^2)
Outer layer	Orthofabric-Teflon/Nomex/Kevlar	0.049
Insulation	Aluminized Mylar-5 —plies	0.014
Spacer	Dacron fiber5—plies	0.011
Inner liner	Teflon	0.028
EVVA shell	Polycarbonate	0.381
Sun visor	Polysulfone	0.190
Eye shade	Polysulfone	0.190
Protective visor	Polycarbonate	0.182
Helmet	Polycarbonate	0.182

The extravehicular gloves are similar except that they do not include cooling tubes. The PLSS, otherwise known as the backpack, consists of the primary oxygen system, oxygen ventilation system, liquid transport system, water feed circuit, secondary oxygen pack (SOP), Extravehicular Mobility Unit (EMU) radio, caution and warning system, contaminant control cartridge (CCC), EMU electrical system, EMU battery, and the display and control module (DCM), which is on the front of the HUT. A listing of these items and their main material constituents and approximate masses is given in Table 1. The overall size of the PLSS unit is approximately 23x25x7 inches. Because of the sensitivity of the eyes, the EVVA consists of numerous visors, which have been constructed to provide maximum protection. Most visors are made of polycarbonate or polysulfone. A list of the different visors and the helmet, and their material composition and areal density is in Table 2.

The commercial CAD software package IDEAS®[12] was used to model the space suit. The effort expended on the modeling was focused on simplicity, but it included an accurate representation of the components that contribute most to radiation shielding,[3] i.e., the visors and the PLSS. An effort was also made to make sure that solid angles subtended by the modeled elements were compatible with those of the actual suit. The current CAD representation of the space suit assembly is shown in Fig.

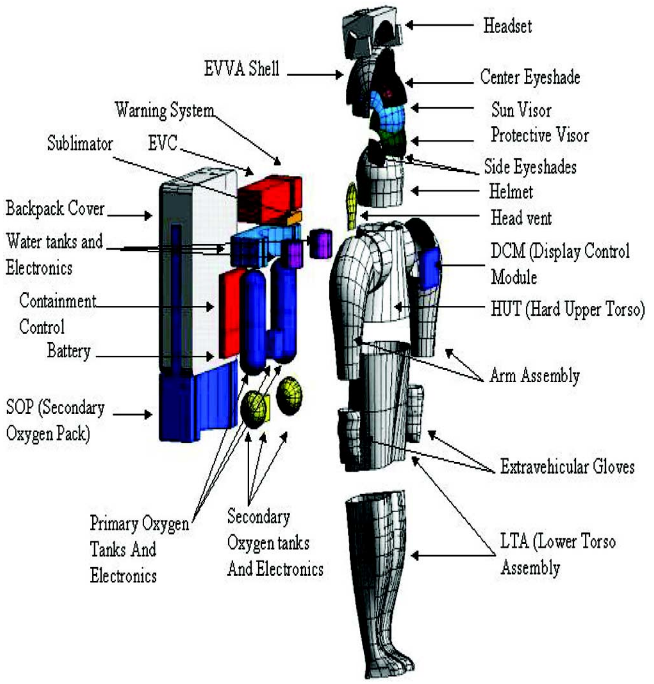

Fig. 3. Computer-aided design (CAD) model of the U.S. Space Shuttle EVA spacesuit.[11)]

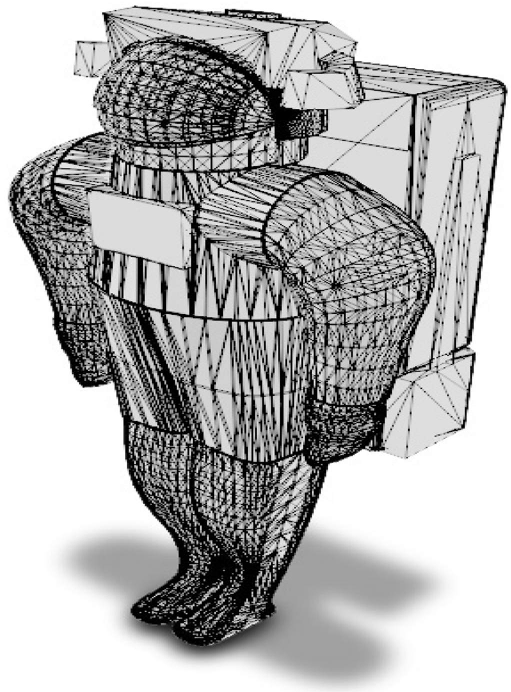

Fig. 4. Finite element model (FEM) of the U.S. Space Shuttle EVA spacesuit.[11)]

Table 3. Description of CAD modeled space suit components.

Components	Mass (kg)	Model volume (cc)	Computed ensity (g/cc)	Composition (atom fraction)
HUT	3.52	2,393	1.47	0.18 H, 0.14 C, 0.02 N, 0.42 O, 0.04 F, 0.19 Si
DCM	5.52	2,760	2.00	0.27 H, 0.31 C, 0.16 O, 0.05 Si, 0.16 Fe, 0.05 Cu
Arm assembly	1.62	1,857	0.872	0.47 H, 0.37 C, 0.05 N, 0.11 O, 0.07F, 0.003 Cl
EVA gloves	0.276	316	"	"
LTA	2.88	3,300	"	"
Legs (ea.)	1.43	1,641	"	"
Headset	3.6	6,984	0.515	0.35 H, 0.41 C, 0.18 O, 0.053 Si
EVVA shell	1.49	1,244	1.2	0.42 H, 0.37 C, 0.09 O
Cen. eyeshade	0.66	364	1.8	0.66 O, 0.33 Si
Sun visor	0.44	353	1.24	0.41 H, 0.50 C, 0.07 O, 0.02 S
Prot. visor	0.43	366	1.2	0.42 H, 0.37 C, 0.09 O
Helmet	0.61	505	1.2	0.42 H, 0.37 C, 0.09 O
Side visors, each	0.065	35	1.8	0.66 O, 0.33 Si
Head vent	0.12	99	1.2	0.42 H, 0.37 C, 0.09 O
EVC	9.02	7,800	1.16	0.34 H, 0.39 C, 0.17 O, 0.05 Si, 0.05 Cu
Warning system	2.64	2,280	1.16	"
Sublimator	1.6	1,600	1	0.67 H, 0.33 O
Water tanks (each)	1.1	1,099	1	0.67 H, 0.33 O
Water S&C	8.35	7,220	1.16	0.27 H, 0.31 C, 0.16 O, 0.05 Si, 0.16 Fe, 0.05 Cu
Prim.O& cont	12.8	11,002	1.16	0.24 H, 0.28 C, 0.14 O, 0.04 Si, 0.22 Fe, 0.08 Cu
Sec.O tanks	1.29	1,643	0.782	0.19 Cr, 0.71 Fe, 0.10 Ni
Back cover	9.8	7,568	1.29	0.42 H, 0.37 C, 0.09 O
Contam. cont.	2.89	2,760	1.05	0.33 H, 0.33 Li, 0.33 O
Battery	4.48	1,200	3.73	0.33 O, 0.33 Zn, 0.33 Ag
Sec.O tanks	7.61	23,416	0.325	0.27 H, 0.31 C, 0.16 O, 0.05 Si, 0.16 Fe, 0.05 Cu

3. Once the solid CAD model of the suit was complete, a finite element model (FEM) was applied to it. This model consisted of 28 components representing the different elements of the suit, visors, and PLSS. Because of the complexity of the model, the finite element model has over 30,000 facets. This FEM was then used in the ray-tracing procedure to determine the directional shielding at a given target point. In Fig. 4 it is shown the FEM of the Shuttle EVA Spacesuit. This modeling effort is described in full detail in Refs. 1, 3 and 11.

For the various space suit components, values for the density are obtained as averages. But for the LCVG, an average areal density taken only from the values for the fabric is inaccurate because the water-filled tubes cover approximately 40% of the surface area. This results in an inhomogeneous structure that can't be well represented by only the fabric mean areal density. In a model of the actual fabric/tube transmission properties, the water-filled tube geometry must be dealt with specifically by the transport through actual material layers as opposed to assuming homogeneity and by the performance of particle transport experiments to provide data for the development of models of inhomogeneities within the fabric. These tasks were performed at the LBNL 88″ cyclotron with a 35 MeV proton beam, and the fabric transmission properties are represented as an analytical model that has good agreement with low-energy proton transmission testing.[13] The fabric is best fitted as a normal distribution of material of mean thickness of 0.161 ± 0.03 g/cm^2 of material, with its mean areal density without cooling tubes being 0.185 g/cm^2.

The chemical composition for this, as for all other space suit components, needed to be known, but in the transport codes used in the analysis, it needed to be limited to only six atomic elements. Table 3 lists each component along with its modeled composition and mass properties. When the CAD model mass is compared to the actual mass of the suit, the PLSS and the EVVA mass estimates are close. For the space suit assembly (SSA) itself, the values are much lower. This is believed to be because the disconnects for the gloves, the HUT, and the arm assembly have not been built into the model, a result of their small solid angles.[3,11]

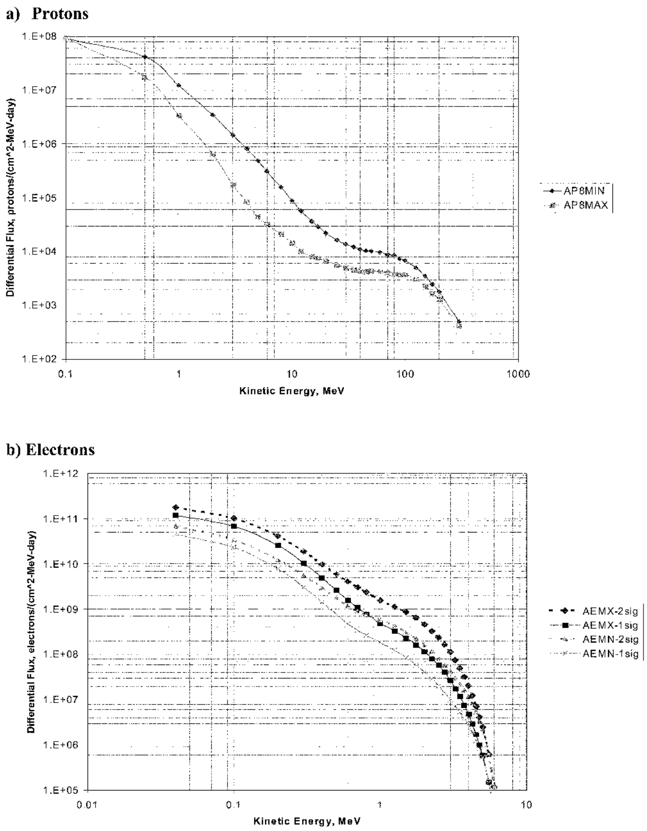

Fig. 5. Differential flux spectra of solar minimum and maximum for trapped protons (a) and electrons (b).[3,11]

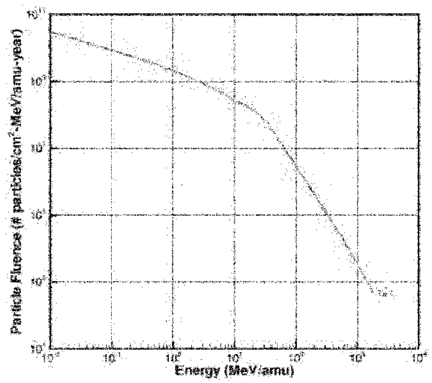

Fig. 6. Spectrum of the solar particle event of September 29, 1989.[13]

RADIATION ENVIRONMENTS

The radiation environments to be considered are the LEO trapped radiation environment for ISS EVA scenarios and solar particles for deep-space exposures. For the LEO environment, the electron and proton trapped fluxes modeled in the standard NASA AE8 and AP8 models of the NASA-GSFC National Space Science Data Center have been used, as provided by the SPace ENVironment Information System (SPENVIS).[14] The differential energy spectra in Fig. 5 (a and b) are shown as omnidirectional fluxes and in transport calculations have been assumed to be isotropic. The orbital conditions have been specified as 400 km altitude with an inclination angle of 51.6°, nominally applicable to ISS, and with flux levels pertaining to orbit-averaged quantities. The solar maximum and minimum spectra approximately define an envelope of extremes for normal solar conditions. The SPENVIS 1- and 2-sigma electron spectra have been used in the calculations for the more variable electron fluxes, which are taken to represent confidence levels of 68% and 97%. It should be noted that maximum electron fluxes tend to occur near solar maximum conditions, whereas the opposite is true for trapped protons.

For the solar particles, a spectrum with particle fluxes equivalent to four times the intensity of the September 29, 1989, event,

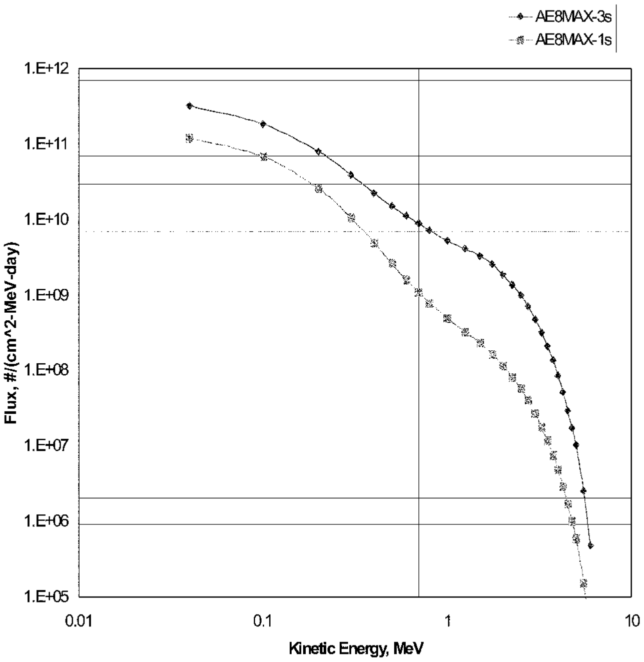

Fig. 7. Orbit-averaged electron flux for nominal and simulated storm conditions.[11)]

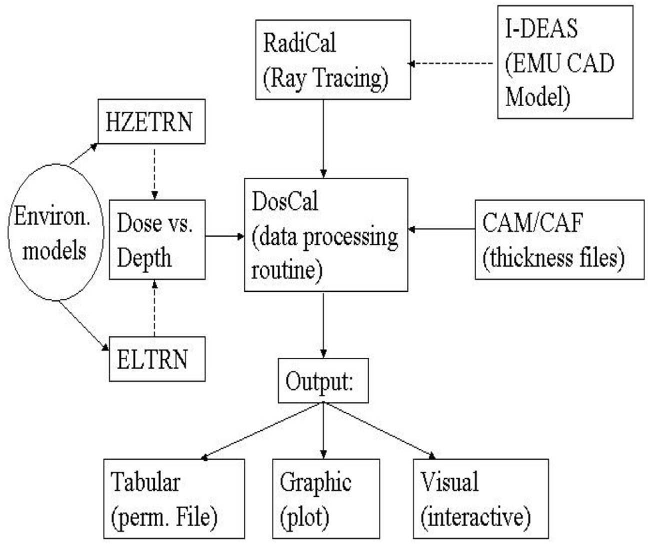

Fig. 8. Layout of the computational method used in the analysis.[11)]

shown in Fig. 6,[15)] has been adopted for protons, and a simulated storm environment for electrons has been generated through the AE8MAX model for the 3-sigma confidence level, as given by SPENVIS,[14)] for nominal ISS orbital conditions. The only rationale for this choice is the rough correspondence between the 3-sigma confidence level and the approximate frequency of severe storms per solar cycle reported by the NOAA Space Environment Laboratory,[16)] and it relates to their K_p space weather index value of 8 to 9. Comparisons between the 1-sigma and 3-sigma flux distributions are shown in Fig. 7.

HUMAN BODY GEOMETRY MODEL

The model used to represent astronaut body geometry for dose assessment is the Computerized Anatomical Male (CAM) model, first developed by Kase[17)] in 1970, then corrected in combinatorial geometry[7)] in 1973 to represent the 50th percentile USAF male. This detailed model comprises some 1,100 unique geometric surfaces and some 2,400 solid regions. The internal body geometry such as critical body organs, voids, bone, and bone marrow are explicitly modeled with the proper chemical composition and density. To take into account the increasing number of female astronauts, the Computerized Anatomical Female (CAF) was later developed by Yucker and Huston[8,18)] and refined by Atwell1.[9,20)] Since the average female is approximately 92% the size of the average male, the CAF was rescaled accordingly from the CAM, with the male organs removed and replaced with female organs (breast, uterus, ovaries). A 3-D scaling capability has been added to both models for the consideration of different astronaut sizes. With a ray-tracing procedure, it is possible to generate shielding distributions for any point within and on model surfaces; these points have been already extensively used to obtain body exposures for Shuttle and ISS astronauts.[3)]

RADIATION TRANSPORT

The general layout of the computational method used in this work is sketched in Fig. 8. The solid geometry data provided by the CAD model of the space suit residing in the IDEAS® commercial software are processed by the RadICal ray-tracing procedure[21)] to generate a file containing values for thickness of materials along rays directed at a chosen target point within the CAD model. The thickness file includes the distance of each material traversed in order, progressing from the outer boundary inward toward the target point. After the selection of the pertinent environmental models to specify the charged particle flux boundary conditions, the relevant transport codes are used to generate dose vs. depth functions for each material under consideration over a range of thicknesses adequate for interpolation.

Transport calculations for protons in the modeled materials were carried out by using a current version of the NASA Langley Research Center (LaRC) heavy ion deterministic code HZETRN.[22)] This version provides particle energy spectra as well as the pertinent dosimetric quantities at predefined positions in the material layer of interest, with energy deposition from both primary and secondary particles, including nuclear target fragments, accounted for. Electron transport calculations were performed by using a deterministic code, ELTRN, recently developed at LaRC,[23)] which also provides estimates of the exposures from energetic secondary photons (bremsstrahlung). For shielding thicknesses comparable to those of the space suit, bremsstrahlung exposures in LEO are known to always be much smaller than those from charged particles.[11)] Depth-dose profiles

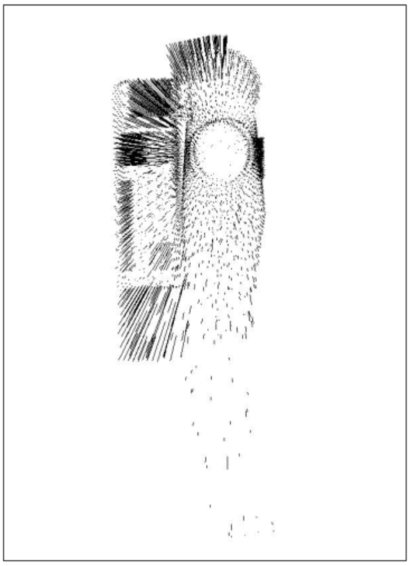

Fig. 9. Projected space suit material thicknesses along 968 ray directions about a point in the sternum.[3)]

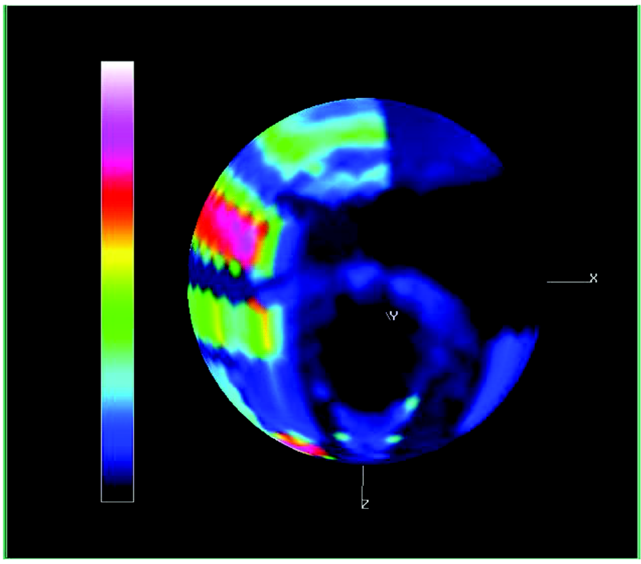

Fig. 10. Spherical visualization of the space suit shielding distribution about a point in the sternum (relative shielding color coding).[3)]

for trapped protons, electrons and bremsstrahlung photons are shown in Fig. 9.

From transport computation examples[11)] for selected space suit materials, computed with peak flux conditions for protons (solar minimum) and electrons (solar maximum) as boundary conditions, it is inferred that the thickness values of 1 or 2 g/cm^2 are most important for the EVA suit, though the thicknesses for some directions at certain target points can be somewhat less or much greater. It is seen that significant dose levels (> ~0.01 cSv/day) for protons can occur for thicknesses well in excess of 10 g/cm^2, but electrons produce little or no exposure for thicknesses above ~2.5 g/cm^2. It is also noteworthy that the dose variations resulting from different material densities are much greater for electrons in the thickness range of interest.

The special characteristics of the LCVG transmission properties, with its composition of a relatively thin fabric interlaced with water-filled acetate cooling tubes and with the large exposure variations that can occur on a small scale, have been incorporated with an algorithm based on a random sampling procedure (along with some geometric complexity). A fully detailed description of the LCVG model is given in Ref. 3 and an analysis of its effects on radiation transport in Ref. 11. This analysis shows an increase in skin dose and dose at depth with respect to the mean LCVC average density model, which suggests that the space suit fabric is less effective in protecting skin and body from radiation than previously assumed.

RESULTS

The dose at a location within the astronaut's body is evaluated by considering the surrounding shielding by the space suit materials and body tissues. For a given point in the target, the space suit material distribution was evaluated along 968 ray directions.

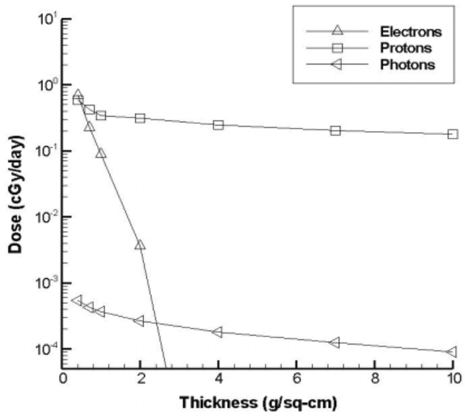

Fig. 11. Depth-dose curves for trapped protons, electrons and bremsstrahlung photons.

This distribution was chosen to match the ray distribution used in the CAM data,[21)] each one with a fixed solid angle ($\Delta\Omega = 4\pi/968$). To better understand these distributions and their effects, two methods have been used to visualize the results of the ray tracing. The first is the visualization of the rays as they intersect the material throughout the suit. In the example in Fig. 10, the projected rays through the space suit materials in and around a point in the sternum is shown, with the shielding role of the EMU lights and camera, the backpack, and the DCM clearly evident. Another visualization technique is the projection on a sphere by a color scale of the relative shielding within the suit around the dose point, as shown in Fig. 11. If the sphere is fully rotated, the shielding in the total solid angle from every ray direction is examined. The power of these techniques is assessed in Ref. 21. To obtain results representative of the whole human body without actually performing the analysis for the entire set

Table 4. Results for space suit with LCVG modeled as a mono-layer fabric.

a) Proton daily doses received at a given target point

	PDEMN	PDEMX	PDOMN	PDOMX
Shin	0.0175	0.0078	0.0115	0.0054
Thigh	0.0184	0.0079	0.0119	0.0054
Chest	0.0118	0.0057	0.0081	0.0041
Pelvis	0.0024	0.0018	0.0017	0.0013
Sternum	0.0042	0.0028	0.0031	0.0020
Thyroid	0.0086	0.0047	0.0062	0.0034
Colon	0.0035	0.0024	0.0026	0.0017
Testes	0.0060	0.0035	0.0044	0.0026
Lens	0.0095	0.0052	0.0069	0.0038

b) Electron daily doses received at a given target point

	EDMN1	EDMN2	EDMX1	EDMX2	EDMX3
Shin	0.1287	0.4483	0.3477	1.3217	5.1174
Thigh	0.1567	0.5918	0.4247	1.6068	6.1944
Chest	0.0472	0.1826	0.1258	0.4861	1.9120
Pelvis	0	0	0	0	0
Sternum	0	0	0	0	0
Thyroid	0.0040	0.0163	0.0094	0.0391	0.1625
Colon	0	0	0	0	0
Testes	0	0	0	0	0
Lens	0.0010	0.0040	0.0020	0.0085	0.0356

Table 5. Results for space suit with LCVG modeled with its tube structure.

a) Proton daily doses received at a given target point

	PDEMN	PDEMX	PDOMN	PDOMX
Shin	0.0334	0.0135	0.0213	0.0092
Thigh	0.0323	0.0130	0.0205	0.0088
Chest	0.0914	0.0091	0.0134	0.0065
Pelvis	0.0245	0.0110	0.0167	0.0077
Sternum	0.0192	0.0092	0.0136	0.0067
Thyroid	0.0198	0.0092	0.0135	0.0065
Colon	0.0233	0.0106	0.0160	0.0075
Testes	0.0252	0.0112	0.0171	0.0079
Lens	0.0168	0.0084	0.0119	0.0061

b) Electron daily doses received at a given target point

	EDMN1	EDMN2	EDMX1	EDMX2	EDMX3
Shin	0.3020	1.1360	0.8182	3.0842	11.853
Thigh	0.2956	1.1041	0.8025	3.0043	11.475
Chest	0.0809	0.3093	0.2163	0.8271	3.2218
Pelvis	0.1371	0.5415	0.3665	1.4481	5.8008
Sternum	0.0493	0.2003	0.1266	0.5147	2.1137
Thyroid	0.0892	0.3336	0.2405	0.8999	3.4480
Colon	0.1145	0.4544	0.3048	1.2098	4.8661
Testes	0.1425	0.5581	0.3801	1.4897	5.9279
Lens	0.0252	0.0974	0.0660	0.2560	1.0075

Table 6. Abbreviation description list for Tables 4 and 5.

Abbreviation	Description
PDEMN	Proton dose equivalent (cSv) during solar minimum
PDEMX	Proton dose equivalent (cSv) during solar maximum
PDOMN	Proton dose (cGy) during solar minimum
PDOMX	Proton dose (cGy) during solar maximum
EDMN1	Electron dose (cGy) during solar minimum (1 sigma)
EDMN2	Electron dose (cGy) during solar minimum (2 sigma)
ENMX1	Electron dose (cGy) during solar maximum (1 sigma)
ENMX2	Electron dose (cGy) during solar maximum (2 sigma)
ENMX3	Electron dose (cGy) during solar maximum (3 sigma)

Table 7. Organ dose equivalent limits (Sv) for all ages, as recommended by NCRP (data from Ref. 24).

	BFO (Sv)	Eye (Sv)	Skin (Sv)
Monthly (30 Days)	0.25	1.0	1.5
Annual	0.50	2.0	3.0
Career	See below	4.0	6.0

Career whole-body dose equivalent limits (Sv) for a 3% lifetime excess risk of fatal cancer as a function of the age at exposure, as recommended by NCRP (data from Ref. 24).

Age	25	35	45	55
Male	0.7	1.0	1.5	2.9
Female	0.4	0.6	0.9	1.6

of the 147 CAM data points, the analysis was limited to nine points, namely, three skin points (shin, thigh, and chest), two Blood- Forming Organ (BFO) points (pelvis and sternum), and four organ points (thyroid, colon, testes, and lens). These nine points were then run through the electron transport code, ELTRN, for solar minimum and maximum conditions for one, two, and three (storm scenario, which is discussed previously) sigma. These points were also run through the proton code, HZETRN, for solar minimum and maximum conditions. Two space suit layouts are considered in the computation with the LCVG fabric viewed as a monolayer average density fabric and the tube structure of the LCVG resulting in shielding nonuniformities. The results are shown in Table 4 (a, b) and Table 5 (a and b), with the explanation of the abbreviations given in Table 6. By comparing Table 4b to Table 5b, we see that the self-shielding of the body contributes significantly to protecting the BFO and other organs from the trapped electron radiation, whereas the suit itself does not provide much protection. The trapped proton radiation is much less intense at the skin point locations compared to the electron radiation, but it does penetrate through the body and constitutes most of the dose received by internal organs. All results are to be compared with the dose limits recently proposed by NCRP,[24] shown in Table 7.

CONCLUSIONS

A computational technique is now available for detailed and comprehensive astronaut space radiation exposure evaluations for EVA scenarios. Code validation and streamlining have been performed to the extent that full implementation with the space suit/CAM-CAF combination may be carried out for a distribution, or grid, of target points throughout the configuration. The results for astronaut exposures can be obtained for the full set of CAM points in a short time, only minutes on an average computational speed serial machine such as a 300 MHz DEC/ALPHA station.[11]

The purpose of the present work is to provide a means for generating accurate and comprehensive exposure evaluations in a time frame that allows a more or less immediate application, as opposed to one after the fact, i.e., scenarios with time-varying external environments, assessment, and optimization of the effect of space suit modifications on shielding properties. It is clear from the present analysis and results that the space suit has some important features that will have some benefit in reducing the health risks of astronauts under the extreme exposure conditions in space. Even so, the space suit's design reveals some weakness with respect to radiation protection, which is already clear. Mainly, attention has been given to the space suit fabric, which is less effective in protecting the skin from exposure than previously assumed and which could be greatly improved.[3,11,13,25,26] It is clear that even modest additions to, replacements of, and changes in the fabric elements could have very important effects, resulting in a greatly improved protection of crew members engaged in EVA.[3,25,26]

REFERENCES

1. Ross, A. J., Webbon, B., Simonsen, L. C., and Wilson, J. W. (1997) Spacesuits. In: Shielding Strategies for Human Space Exploration, Eds. Wilson, J. W., Miller, J., Konradi, A. and Cucinotta, F. A., Chap. 14, p. 283, NASA Conference Publication CP-3360.
2. Wilson, J. W., Cucinotta, F. A., Shinn, J. L., Simonsen, L. C., Dubey, R. R., Jordan, W. R., Jones, T. D., Chang, C. K. and Kim, M. Y. (1999) Shielding from solar particle event exposures in deep space. Radiat. Meas. **30**, 361.
3. Anderson, B. M., Nealy, J. E., Qualls, G. D., Staritz, P. J., Wilson, J. W., Kim, M. H. Y., Cucinotta, F. A., Atwell, W., De Angelis, G., Ware, J. and Persans, A. E. (2001) Shuttle spacesuit (radiation) model development. Paper No. 2001-01-2368 in Proc. 31st International Conf. On Environmental Systems (ICES), Orlando, FL, July 9-12, 2001.
4. Suzuki, S., Miura, Y., Mizuno, S. and Furusawa, Y. (2002) Models for mixed irradiation with a 'reciprocal-time' pattern of the repair function. J. Radiat. Res. **43**, 257.
5. Goodhead, D. T. (1999) Mechanisms for the biological effectiveness of high-LET radiations. J. Radiat. Res. **40**, S1.
6. Antonelli, F., Bettega, D., Calzolari, P., Cherubini, R., Dalla Vecchia, M., Durante, M., Favaretto, S., Grossi, G., Marchesini, R., Pugliese, M. G., Scampoli, P., Simone, G., Sorrentino, E.., Tabocchini, A., Tallone, L. and Tiveron, P. (2001) Inactivation of human cells exposed to fractionated doses of low energy protons: relationship between cell sensitivity and recovery efficiency. J. Radiat. Res. **42**, 347.
7. Billings, M. P. and Yucker, W. R. (1973) The Computerized Anatomical Man (CAM) Model. Report MDC G4655, McDonnell Douglas Corporation, Huntington Beach, CA.
8. Yucker, W. R. and Huston, S. L. (1990) Computerized Anatomical Female (CAF). Final Report. Report MDC H 6107, McDonnell Douglas Corporation, Huntington Beach, CA.
9. Yasuda, H. and Fujitaka, K. (2001) Cosmic radiation protection dosimetry using an electronic personal dosemeter (Siemens EPD) on selected internal flights. J. Radiat. Res. **42**, 57.
10. Kramer, M. (2001) Treatment planning for heavy-ion radiotherapy: Biological optimization of multiple beam ports. J. Radiat. Res. **42**, 39.
11. Anderson, B. M., Nealy, J. E., Wilson, J. W. and Simonsen, L. (2002) CAD model of astronaut radiation exposures during EVA: nominal and extreme scenarios. Paper No. 2002-02-2458 in Proc. 32st International Conf. On Environmental Systems (ICES), San Antonio, TX, July 15-18, 2002.
12. IDEAS" CAD software package at the Electronic Data Systems (EDS) company website (available at http://www.eds.com/products/plm/ideas/version10.shtml), last accessed Feb. 25, 2003.
13. Wilson, J. W., Tweed, J., Zeitlin, C., Kim, M. H. Y., Anderson, B. M., Cucinotta, F. A., Ware, J. and Persans, A. E. (2001) Shuttle spacesuit fabric/LCVG model validation. Paper No. 2001-01-2372 in Proc. 31st International Conf. On Environmental Systems (ICES), Orlando, FL, July 9-12, 2001.
14. SPENVIS website, i.e. ESA/ESTEC SPace ENVironment Information System: (available at http://www.spenvis.oma.be/spenvis/), last accessed Mar. 7, 2002.
15. Tripathi, R. K., Wilson, J. W., Cucinotta, F. A., Nealy, J. E., Clowdsley, M. S. and Kim, M.-H. K. (2001) Deep space mission radiation shielding optimization. Paper No. 2001-01-2326 in Proc. 31st International Conf. On Environmental Systems (ICES), Orlando, FL, July 9-12, 2001.
16. NOAA Space Environment Laboratory website (available at http://www.sel.noaa.gov), last accessed Mar. 7, 2002.
17. Kase, P. G. (1970) Computerized anatomical model man. Report AFWL-TR-69-161, Air Force Weapons Laboratory, Kirtland Air Force Base, NM.
18. Yucker, W. R. (1992) Computerized anatomical female body self-shielding distributions. Report MDC 92H0749, McDonnell Douglas Corporation, Huntington Beach, CA.
19. Atwell, W. (1992) Anatomical models for space radiation application: an overview. Invited Paper No. F2.4-M.1.06 presented at the Committee on Space Research (COSPAR), Washington, DC, August 28-September 5, 1992.
20. Atwell, W., Hardy, A. C. and Peterson, L. (1994) Organ radiation doses and lifetime risk of excess cancer for several Space Shuttle missions. Invited Paper No. F2.4-001 presented at the Committee on Space Research (COSPAR), Hamburg, Germany, July 11-21, 1994.

21. Qualls, G. D. and Boykin, R. (1997) Space radiation shielding analysis by CAD techniques. In: Shielding Strategies for Human Space Exploration, Eds. Wilson, J. W., Miller, J., Konradi, A. and Cucinotta, F. A., Chap. 17, p. 365, NASA Conference Publication CP-3360.
22. Wilson, J. W., Badavi, F. F., Cucinotta, F. A., Shinn, J. L., Badhwar, G. D., Silberberg, R., Tsao, C. H., Townsend, L. W. and Tripathi, R. K. (1995) HZETRN: description of a free-space ion and nucleon transport and shielding computer program. NASA Technical Paper TP-3495.
23. Nealy, J. E., Anderson, B. M., Cucinotta, F. A., Wilson, J. W., Katz, R. and Chang, C. K. (2002) Transport of space environment electrons: a simplified rapid-analysis computational procedure. NASA Technical Paper TP 2002-211448.
24. NCRP (2001) Radiation protection guidance for activities in low-Earth orbit, National Council on Radiation Protection and Measurements, Publication N. 132, Bethesda MD.
25. Ware, J., Ferl, J., Wilson, J. W., Clowdsley, M. S., De Angelis, G., Tweed, J. and Zeitlin, C. G. (2002) Design and testing of improved spacesuit shielding components. Paper No. 2002-02-2462 in Proc. 32st International Conf. On Environmental Systems (ICES), San Antonio, TX, July 15n18, 2002.
26. Ware, J., Ferl, J., Wilson, J. W., Clowdsley, M. S., De Angelis, G., Tweed, J. and Zeitlin, C. G. (2002) Test results of improved spacesuit shielding materials components. Paper No. 2003-02-338 in Proc. 33st International Conf. On Environmental Systems (ICES), Vancouver, BC, Canada, to be held in July 2002.

Received on July 24, 2002
Accepted on February 6, 2003